Journal of Solid State Chemistry 183 (2010) 712–719

Contents lists available at ScienceDirect

Journal of Solid State Chemistry

journal homepage: www.elsevier.com/locate/jssc

Phase formation features in the systems M_2MoO_4–$Fe_2(MoO_4)_3$ (M=Rb, Cs) and crystal structures of new double polymolybdates $M_3FeMo_4O_{15}$

Klara M. Khal'baeva [a], Sergey F. Solodovnikov [b,c,*], Elena G. Khaikina [a,d], Yuliya M. Kadyrova [a,d], Zoya A. Solodovnikova [b], Olga M. Basovich [a]

[a] Baikal Institute of Nature Management, Siberian Branch, Russian Academy of Sciences, Sakh'yanova St. 6, Ulan-Ude, 670047 Buryat Republic, Russia
[b] Nikolaev Institute of Inorganic Chemistry, Siberian Branch, Russian Academy of Sciences, Akad. Lavrent'ev Ave. 3, Novosibirsk 630090, Russia
[c] Novosibirsk State University, Pirogov St. 2, Novosibirsk 630090, Russia
[d] Buryat State University, Smolin St. 24a, Ulan-Ude, 670000 Buryat Republic, Russia

ARTICLE INFO

Article history:
Received 11 September 2009
Received in revised form
29 December 2009
Accepted 10 January 2010
Available online 18 January 2010

Keywords:
Alkali metal
Iron
Phase formation
Non-quasibinary join
Double polymolybdate
Crystal structure

ABSTRACT

The systems M_2MoO_4–$Fe_2(MoO_4)_3$ (M=Rb, Cs) were shown to be non-quasibinary joins of the systems M_2O–Fe_2O_3–MoO_3. New compounds $M_3FeMo_4O_{15}$ were revealed along with the known $MFe(MoO_4)_2$ and $M_5Fe(MoO_4)_4$. The unit cell parameters of the new compounds are a=11.6192(2), b=13.6801(3), c=9.7773(2) Å, β=92.964(1)°, space group $P2_1/c$, Z=4 (M=Rb) and a=11.5500(9), b=9.9929(7), c=14.513(1) Å, β=90.676(2)°, space group $P2_1/n$, Z=4 (M=Cs). In the structures of $M_3FeMo_4O_{15}$ (M=Rb, Cs), a half of the FeO_6 octahedra share two opposite edges with two MoO_6 octahedra linked to other FeO_6 octahedra through the bridged MoO_4 tetrahedra by means of the common oxygen vertices to form the chains along the a axis. The difference between the structures is caused by diverse mutual arrangements of the adjacent polyhedral chains.

1. Introduction

Double molybdates of alkali and trivalent metals are well known in literature and belong to the most numerous and studied family of molybdates having important properties and applications. For example, double molybdates with the general formula $MRE(MoO_4)_2$ (where M—alkali metal, RE—trivalent rare earth) are excellent RE-doped laser hosts [1]. By now solid-phase synthesis and flux crystallization techniques were developed for the most of the double molybdates of alkali and trivalent metals; their crystal structures, polymorphism features, and some physical properties [2–4] were investigated. $T-x$ diagrams were constructed for many of the systems in which these phases form, particularly, for the systems containing lanthanides, chromium, and aluminum [3,5–7].

Less attention was devoted to the alkali metal molybdate–iron (III) molybdate systems. Double molybdates $MFe(MoO_4)_2$ (M=Li–Cs), $M_3Fe(MoO_4)_3$ (M=Li, K), $M_5Fe(MoO_4)_4$ (M=K, Rb, Cs) [7–19] were described in literature; the crystal structures of $MFe(MoO_4)_2$ (M=Li, Na, K, Rb) [20–25], $Li_3Fe(MoO_4)_3$ [26] and $Rb_5Fe(MoO_4)_4$ [20] were determined. In the structures, the molybdenum atoms are tetrahedrally coordinated while the Fe^{3+} cations usually have the octahedral coordination excluding the structure of the low-temperature $Rb_5Fe(MoO_4)_4$ [20] where the iron atoms are located in square pyramids. Double molybdates $M_5Fe(MoO_4)_4$ (M=K, Rb) were found to be dimorphic [19]. Unlike low-temperature modifications of these compounds [19,20], the structures of high-temperature modifications as well as $Cs_5Fe(MoO_4)_4$ crystallize in the layer structure of palmierite $K_2Pb(SO_4)_2$ [27].

Double molybdates $MFe(MoO_4)_2$ (M=Na, K, Rb) exhibit interesting ferroelastic and antiferromagnetic properties [10–14], and $Li_3Fe(MoO_4)_3$ is considered as a possible positive electrode in lithium cells [16,17]. However, despite detail characterization and attractive functional properties of some double iron(III) molybdates, none T–x diagrams have been constructed for the systems M_2MoO_4–$Fe_2(MoO_4)_3$ (M=Li, Na, K, Rb, Cs) and only lithium and sodium containing systems were studied using X-ray diffraction [7].

It is interesting to note formation of sodium dimolybdate and iron(III) oxide in the system Na_2MoO_4–$Fe_2(MoO_4)_3$ in the range adjacent to Na_2MoO_4 [7]:

$$3Na_2MoO_4+Fe_2(MoO_4)_3 \rightarrow 3Na_2Mo_2O_7+Fe_2O_3 \quad (1)$$

* Corresponding author at: Nikolaev Institute of Inorganic Chemistry, Siberian Branch, Russian Academy of Sciences, Akad. Lavrent'ev Ave. 3, Novosibirsk 630090, Russia. Fax: +7 383 3309489.
E-mail address: solod@niic.nsc.ru (S.F. Solodovnikov).

0022-4596/$ - see front matter © 2010 Elsevier Inc. All rights reserved.
doi:10.1016/j.jssc.2010.01.008

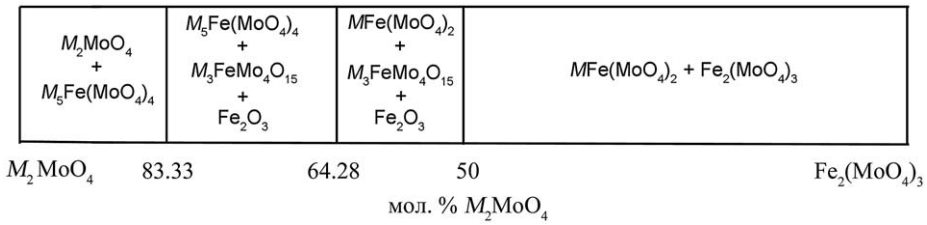

Fig. 1. Phase fields diagram of the M_2MoO_4–$Fe_2(MoO_4)_3$ (M=Rb, Cs) systems.

Table 1
Results of XRD analysis of $0.6Rb_2MoO_4+0.4Fe_2(MoO_4)_3$ sample.[a]

Rb_2MoO_4:$Fe_2(MoO_4)_3$=3:2		$Rb_3FeMo_4O_{15}$[b]		$RbFe(MoO_4)_2$ [35]		Fe_2O_3 [36]	
I/I_0	2θ (deg)	I/I_0	2θ (deg)	I/I_0	2θ (deg)	I/I_0	2θ (deg)
16	11.141	38	11.13				
2	11.798			4	11.815		
20	12.939	48	12.94				
6	13.241	22	13.23				
10	13.766	26	13.77				
9	15.820	20	15.82				
1	16.582	3	16.60				
4	18.046			4	18.056		
1	18.152	3	18.17				
7	18.546	19	18.55				
5	19.307	13	19.32				
		4	19.36				
		3	21.51				
100	21.617			100	21.633		
14	22.367	32	22.37				
5	23.203	15	23.20				
1	23.700			4	23.746		
2	23.896	7	23.91				
12	24.096	33	24.10				
1	24.188					30	24.158
16	25.175	44	25.18				
16	25.287	48	25.29				
16	26.031	43	26.04				
		6	26.05				
37	26.191	100	26.20				
3	26.637	5	26.65				
55	26.746	41	26.75				
		100	26.76				
36	27.622	84	27.64				
3	27.750	9	27.74				
39	28.174	4	28.12				
		89	28.18				
8	28.690	26	28.69				
3	29.443	5	29.44				
51	29.963			69	29.996		
4	30.173	10	30.21				
24	30.300	41	30.30				
19	30.403	24	30.34				
		42	30.41				
15	30.813	35	30.82				
2	30.926	6	30.93				
2	31.317	7	31.33				
52	31.532	6	31.48	48	31.547		
		5	31.59				
2	32.022	7	32.04				
3	32.398	9	32.40				
1	32.995	3	32.99				
3	33.176					100	33.181
2	33.323	4	33.32				
6	33.544	15	33.55				
2	33.761			2	33.786		
3	33.830	7	33.84				
4	34.002	11	34.03				
3	34.383	8	34.39				
2	34.911	8	34.91				
1	35.065	3	35.03				
5	35.143	10	35.16				
		10	35.16				
6	35.250	17	35.26				
2	35.637					70	35.642

[a] The sample sintered at 450 °C for 80 h.
[b] XRD pattern calculated from our single crystal structure data; reflections with $2\theta > 10.5^\circ$ and $I/I_0 \geq 3$ are given.

Thus, the system Na_2MoO_4–$Fe_2(MoO_4)_3$ could be considered as a partial non-quasibinary join of the ternary system Na_2O–Fe_2O_3–MoO_3, since the compositions of $Na_2Mo_2O_7$ and Fe_2O_3 lie outside of the join. In addition, the authors of [28,29] report formation of double polymolybdate $K_3FeMo_4O_{15}$ in the system K_2O–Fe_2O_3–MoO_3. Recently, the crystal structure of $K_3FeMo_4O_{15}$ [30] was determined, which confirms our preliminary data [29]. In the structure, there are polyhedral clusters of two FeO_6 octahedra, four MoO_4 tetrahedra and Mo_2O_7 doubled tetrahedra, which are all joined by the corners. The existence of $K_3FeMo_4O_{15}$ suggests that phase relations in the systems M_2MoO_4–$Fe_2(MoO_4)_3$ with heavy alkali metal molybdates may have more pronounced non-quasibinary character that results in formation of complex oxide (polymolybdate) phases along with double molybdates.

This paper represents our results of a detail study of the phase formation in systems M_2MoO_4–$Fe_2(MoO_4)_3$ (M=Rb, Cs), which were found by us as partially non-quasibinary. We also revealed and structurally studied new compounds $M_3FeMo_4O_{15}$ (M=Rb, Cs).

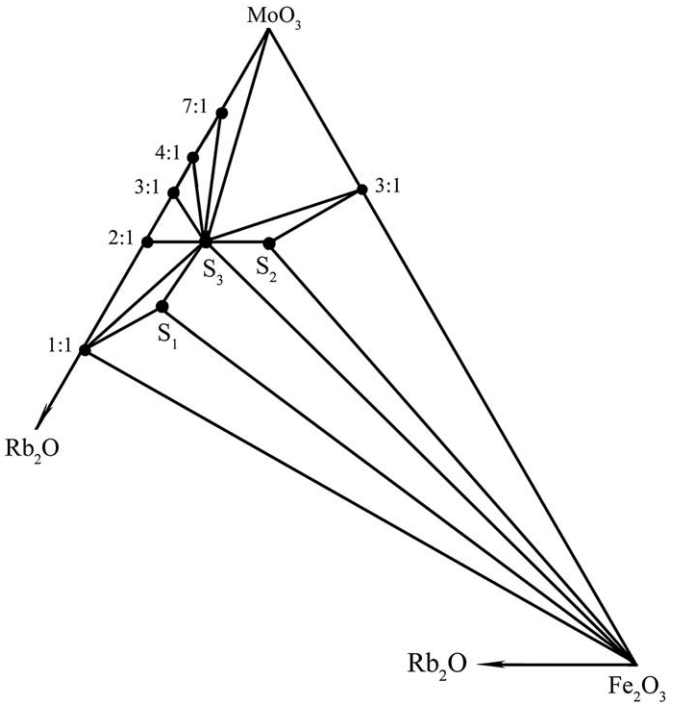

Fig. 2. A possible variant of a partial triangulation of the Rb_2O–MoO_3–Fe_2O_3 system. S_1—$Rb_5Fe(MoO_4)_4$; S_2—$RbFe(MoO_4)_2$; S_3—$Rb_3FeMo_4O_{15}$. Quasibinary character of the joins Rb_2MoO_4–Fe_2O_3, $Rb_5Fe(MoO_4)_4$–Fe_2O_3, $Rb_3FeMo_4O_{15}$–Fe_2O_3, $RbFe(MoO_4)_2$–Fe_2O_3, Rb_2MoO_4–$Rb_5Fe(MoO_4)_4$, $RbFe(MoO_4)_2$–$Fe_2(MoO_4)_3$ were confirmed experimentally.

Table 2
Crystal data and structure refinement details for $Rb_3FeMo_4O_{15}$ and $Cs_3FeMo_4O_{15}$.

Formula	$Rb_3FeMo_4O_{15}$	$Cs_3FeMo_4O_{15}$
Formula weight ($g\,mol^{-1}$)	936.02	1078.34
Crystal system	Monoclinic	Monoclinic
Space group	$P2_1/c$	$P2_1/n$
Unit cell dimensions	a=11.6192(2) Å, b=13.6801(3) Å, c=9.7773(2) Å β=92.964(1)°	a=11.5500(9) Å, b=9.9929(7) Å, c=14.5128(11) Å β=90.676(2)°
V (Å^3); Z	1552.04(5)/4	1674.9(2)/4
Calculated density ($g\,cm^{-3}$)	4.006	4.276
Crystal size, mm	0.15 × 0.12- × 0.10	0.10 × 0.08 × 0.06
μ(Mo$K\alpha$), mm^{-1}	13.473	10.249
θ range (deg) for data collection	1.75–37.57	1.40–30.66
Miller index ranges	$-19 \le h \le 17$, $-22 \le k \le 14$, $-13 \le l \le 16$	$-16 \le h \le 16$, $-14 \le k \le 7$, $-20 \le l \le 20$
Reflections collected/unique	21101/7635 [R(int)=0.0269]	15462/5079 [R(int)=0.0424]
No. of variables	212	213
Goodness-of-fit on F^2 (GOF)	1.033	1.168
Final R indices [$I > 2\sigma(I)$]	$R(F)$=0.0299, w$R(F^2)$=0.0578	$R(F)$=0.0681, w$R(F^2)$=0.1590
R indices (all data)	$R(F)$=0.0475, w$R(F^2)$=0.0616	$R(F)$=0.0738, w$R(F^2)$=0.1642
Extinction coefficient	0.00027(5)	0.00058(9)
Largest difference peak/hole (e Å^{-3})	1.614/−1.337	4.908/−2.480

2. Experimental

As starting reagents commercially available M_2CO_3 (M=Rb, Cs), $Fe(NO_3)_3 \cdot 9H_2O$ and MoO_3 (all of chemical grade) were used. Molybdenum trioxide and M_2CO_3 (M=Rb, Cs) were previously fired at 400–450 °C, and accordance of $Fe(NO_3)_3 \cdot 9H_2O$ to the nominal composition were controlled by chemical and thermogravimetric analyses. Rubidium and cesium molybdates were synthesized by means of calcination of stoichiometric mixtures of the corresponding carbonates and molybdenum trioxide at 400–800 °C for 100 h. Iron(III) molybdate, $Fe_2(MoO_4)_3$, was prepared

Table 3
Selected interatomic distances (Å) for $Rb_3FeMo_4O_{15}$.

Mo(1)—octahedron		**Mo(2)—tetrahedron**	
Mo(1)–O(1)	1.714(2)	Mo(2)–O(7)	1.716(2)
Mo(1)–O(2)	1.717(2)	Mo(2)–O(8)	1.722(2)
Mo(1)–O(3)	1.836(2)	Mo(2)–O(9)	1.803(2)
Mo(1)–O(4)	1.993(2)	Mo(2)–O(4)	1.870(2)
Mo(1)–O(5)	2.267(2)	〈Mo(2)–O〉	1.778
Mo(1)–O(6)	2.535(3)		
〈Mo(1)–O〉	2.010		
Mo(3)—tetrahedron		**Mo(4)—tetrahedron**[a]	
Mo(3)–O(10)	1.715(2)	Mo(4)–O(13)	1.701(2)
Mo(3)–O(6[a])	1.750(2)	Mo(4)–O(14)	1.705(2)
Mo(3)–O(11)	1.791(2)	Mo(4)–O(15)	1.833(2)
Mo(3)–O(12)	1.792(2)	Mo(4)–O(5)	1.890(2)
〈Mo(3)–O〉	1.762	〈Mo(4)–O〉	1.782
Fe(1)—octahedron		**Fe(2)—octahedron**	
Fe(1)–O(5)	1.982(2) × 2	Fe(2)–O(15[a])	1.971(2) × 2
Fe(1)–O(3)	2.003(2) × 2	Fe(2)–O(9[a])	1.998(2) × 2
Fe(1)–O(12)	2.046(2) × 2	Fe(2)–O(11)	2.038(2) × 2
〈Fe(1)–O〉	2.010	〈Fe(2)–O〉	2.002
Rb(1)—polyhedron		**Rb(2)—polyhedron**	
Rb(1)–O(7[b])	2.814(2)	Rb(2)–O(2)	2.846(2)
Rb(1)–O(10[c])	2.917(3)	Rb(2)–O(2[b])	2.932(2)
Rb(1)–O(13[d])	2.931(2)	Rb(2)–O(3[e])	2.942(2)
Rb(1)–O(1[b])	2.989(2)	Rb(2)–O(14)	2.970(2)
Rb(1)–O(3[e])	3.018(2)	Rb(2)–O(12)	3.044(2)
Rb(1)–O(11[e])	3.112(2)	Rb(2)–O(1[e])	3.061(2)
Rb(1)–O(12[e])	3.319(2)	Rb(2)–O(1[b])	3.103(2)
Rb(1)–O(2[e])	3.459(2)	Rb(2)–O(6[e])	3.204(2)
Rb(1)–O(8[f])	3.471(2)	Rb(2)–O(5)	3.643(2)
Rb(1)–O(9[f])	3.689(2)	Rb(2)–O(10)	3.687(3)
〈Rb(1)–O〉	3.172	〈Rb(2)–O〉	3.143
Rb(3)—polyhedron			
Rb(3)–O(8[g])	2.840(2)	Rb(3)–O(7[h])	3.151(2)
Rb(3)–O(9[h])	2.841(2)	Rb(3)–O(7[i])	3.180(2)
Rb(3)–O(8[i])	2.909(2)	Rb(3)–O(14[g])	3.303(2)
Rb(3)–O(15[g])	2.947(2)	Rb(3)–O(13[j])	3.356(3)
Rb(3)–O(10[d])	3.106(3)	〈Rb(3)–O〉	3.070

Symmetry codes: (a) $-x+1, -y, -z+1$; (b) $x, -y+1/2, z+1/2$; (c) $-x+1, -y+1, -z+1$; (d) $x, -y+1/2, z-1/2$; (e) $-x+1, y+1/2, -z+1/2$; (f) $-x+2, y+1/2, -z+1/2$; (g) $x-1, -y+1/2, z-1/2$; (h) $-x+1, -y, -z$; (i) $x-1, y, z$; (j) $x-1, y, z-1$.

[a] Distance Mo(4)–O(4) 2.553(4) Å complements $Mo(4)O_4$ tetrahedron to a trigonal bipyramid.

with a stepwise annealing of equimolar reaction mixture of $Fe(NO_3)_3 \cdot 9H_2O$ and MoO_3 at 400–600 °C for 60 h. Using low-temperature stages of the solid-state synthesis (400–450 °C) excluded MoO_3 volatilization and a departure from the stoichiometric composition. The powder X-ray diffraction patterns of as-prepared anhydrous molybdates agree well with the literature data. Cesium molybdate was isolated in the low-temperature modification while the rubidium compound was in the medium-temperature orthorhombic form due to its high tendency to quenching [31]. The unit cell parameters of $Fe_2(MoO_4)_3$ were consistent with those reported in [32].

Phase formation in subsolidus regions of the systems M_2MoO_4–$Fe_2(MoO_4)_3$ was studied using powder X-ray diffraction (XRD) in the range 350–450 °C for M=Rb and 350–430 °C for M=Cs. The samples containing 90, 83.3, 80, 75, 70, 60, 50, 40 and 20 mol% alkali metal molybdate were prepared by solid-state reactions. The temperature was increased gradually with the step of 30–50 °C and the reaction mixtures were calcinated for 50–100 h at each annealing stage with intermittent grindings in every 20 h. After each annealing stage, powder XRD analysis of the samples was conducted, which followed by changing the thermal treatment regime.

Small crystals of the compounds were grown by spontaneous crystallization of molten ceramic samples or mixtures of constituent molybdates. The heating of ground mixtures, their isothermal holding and slow cooling of the melts at a rate of 4 °C h^{-1} to room temperature were controlled and kept automatically with a ±0.5° accuracy.

Monitoring of solid-state synthesis and phase equilibration were carried out by powder XRD on a D8 ADVANCE Bruker diffractometer (Cu$K\alpha$ radiation, secondary monochromator, maximal 2θ=100°, scan step 0.01–0.02°, exposition 1–10 s). The unit cell parameters were refined by the least-squares method using ICDD program package for preparing experimental standards.

X-ray diffraction data for single crystal structure analysis were collected at room temperature on a Bruker-Nonius X8 Apex CCD area-detector four-cycle diffractometer (Mo$K\alpha$ radiation, graphite monochromator, φ-scans). Data processing was accomplished using SAINT program; an absorption correction was applied with SADABS program [33]. The structures were solved and refined by full-matrix least-squares method on F^2 in anisotropic approximation with SHELX-97 package [34].

Table 4
Selected interatomic distances (Å) for $Cs_3FeMo_4O_{15}$.

Mo(1)—octahedron		**Mo(2)—tetrahedron**	
Mo(1)–O(2)	1.719(10)	Mo(2)–O(8)	1.726(10)
Mo(1)–O(1)	1.725(9)	Mo(2)–O(7)	1.726(10)
Mo(1)–O(3)	1.839(9)	Mo(2)–O(9)	1.795(10)
Mo(1)–O(4)	1.987(9)	Mo(2)–O(4)	1.852(10)
Mo(1)–O(5)	2.337(10)	〈Mo(2)–O〉	1.775
Mo(1)–O(6)	2.494(11)		
〈Mo(1)–O〉	2.017		
Mo(3)—tetrahedron		**Mo(4)—tetrahedron**	
Mo(3)–O(10)	1.719(12)	Mo(4)–O(14)	1.718(10)
Mo(3)–O(6^a)	1.767(10)	Mo(4)–O(13)	1.723(11)
Mo(3)–O(12)	1.773(10)	Mo(4)–O(15)	1.827(11)
Mo(3)–O(11)	1.780(10)	Mo(4)–O(5)	1.858(10)
〈Mo(3)–O〉	1.760	〈Mo(4)–O〉	1.782
Fe(1)—octahedron		**Fe(2)—octahedron**	
Fe(1)–O(5)	1.975(10) × 2	Fe(2)–O(9)	2.001(10) × 2
Fe(1)–O(3)	1.979(10) × 2	Fe(2)–O(15)	2.003(10) × 2
Fe(1)–O(12)	2.066(10) × 2	Fe(2)–O(11^a)	2.016(10) × 2
〈Fe(1)–O〉	2.007	〈Fe(2)–O〉	2.007
Cs(1)—polyhedron		**Cs(2)—polyhedron**	
Cs(1)–O(1^b)	3.032(10)	Cs(2)–O(2)	2.929(11)
Cs(1)–O(10^c)	3.071(12)	Cs(2)–O(9^f)	3.042(10)
Cs(1)–O(7^b)	3.091(10)	Cs(2)–O(8^b)	3.058(11)
Cs(1)–O(13^d)	3.102(13)	Cs(2)–O(14)	3.157(11)
Cs(1)–O(11^e)	3.161(11)	Cs(2)–O(7^b)	3.271(12)
Cs(1)–O(3^e)	3.225(9)	Cs(2)–O(7^f)	3.284(11)
Cs(1)–O(8^f)	3.294(11)	Cs(2)–O(12)	3.297(10)
Cs(1)–O(2^e)	3.450(11)	Cs(2)–O(6^f)	3.627(11)
Cs(1)–O(12^e)	3.477(10)	Cs(2)–O(13^d)	3.667(13)
Cs(1)–O(9^f)	3.574(10)	Cs(2)–O(10)	3.826(15)
〈Cs(1)–O〉	3.248	〈Cs(2)–O〉	3.316
Cs(3)—polyhedron			
Cs(3)–O(3^g)	3.073(9)	Cs(3)–O(1)	3.259(10)
Cs(3)–O(8^d)	3.078(10)	Cs(3)–O(1^g)	3.259(11)
Cs(3)–O(2)	3.127(10)	Cs(3)–O(10^h)	3.454(14)
Cs(3)–O(15^d)	3.201(11)	Cs(3)–O(13^i)	3.459(13)
Cs(3)–O(14^d)	3.215(11)	Cs(3)–O(6^g)	3.562(12)
〈Cs(3)–O〉	3.269		

Symmetry codes: (a) $-x+1, -y+1, -z$; (b) $-x+1/2, y+1/2, -z+1/2$; (c) $-x+1, -y+1, -z+1$; (d) $-x+1/2, y-1/2, -z+1/2$; (e) $x-1/2, -y+1/2, z+1/2$; (f) $x+1/2, -y+1/2, z+1/2$; (g) $-x+1, -y, -z$; (h) $-x+3/2, y-1/2, -z+1/2$; (i) $x, y-1, z$.

3. Results and discussion

3.1. Phase formation in M_2MoO_4–$Fe_2(MoO_4)_3$ (M=Rb, Cs) systems

The studies on the systems M_2MoO_4–$Fe_2(MoO_4)_3$ (M=Rb, Cs) confirmed formation of double molybdates $MFe(MoO_4)_2$ and $M_5Fe(MoO_4)_4$ described in literature. The lattice parameters of $RbFe(MoO_4)_2$ (a=5.6748(2), c=7.5038(5) Å) and $CsFe(MoO_4)_2$ (a=5.6195(2), c=8.0697(3) Å) prepared by us agree well with those reported in [20,24,25,35] for the first compound and slightly correct the parameters determined for the second phase in [7]. A rubidium-containing sample of 5:1 composition quenched from 450 °C in air, was obtained in the low-temperature form whose structure was recently determined in [20]. With increasing the iron content we observed stabilization of the high-temperature modification that results in fixing $Rb_5Fe(MoO_4)_4$, along with other phases, as a mixture of two modifications. The synthesized $Cs_5Fe(MoO_4)_4$ possesses a palmierite-like structure. We failed to prepare single crystals of the palmierite-like phases since none of the numerous growth experiments gave a positive result.

According to XRD data, the phase relations in the systems M_2MoO_4–$Fe_2(MoO_4)_3$ (M=Rb, Cs) within the 0–50 mol% range of M_2MoO_4 are rather simple. XRD patterns of the equilibrated samples show only the lines of boundary compounds $MFe(MoO_4)_2$

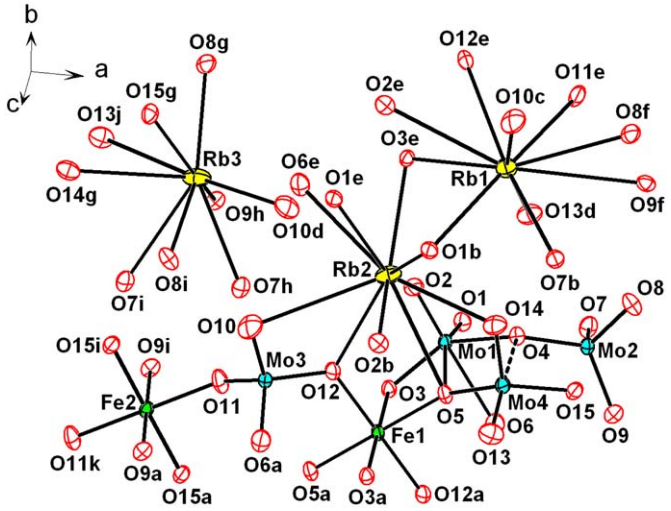

Fig. 3. The asymmetric unit of $Rb_3FeMo_4O_{15}$ structure. Atomic displacement ellipsoids are shown at 50% probability level. Symmetry codes correspond to those given in Table 3, the additional code: (k) $-x, -y, -z+1$.

and $Fe_2(MoO_4)_3$ with reflection intensities corresponding to the relative content of these phases in the reaction mixtures.

An interpretation of the experimental results obtained in the range close to rubidium molybdate is significantly complicated. XRD powder patterns of the samples in the range $M_5Fe(MoO_4)_4$–$MFe(MoO_4)_2$ yield the reflections, which we failed to identify at the first stage of the study. Moreover, none of the samples studied show the reflections of the revealed phase solely that would witness of violating a quasibinarity for these joins. Note that the unidentified reflections have not been assigned to the known rubidium or cesium polymolybdates involved in the ICDD PDF-2 Database. This suggests the formation of double polymolybdates of heavy alkali metals and iron(III) in the oxide systems M_2O–MoO_3–Fe_2O_3 (M=Rb, Cs).

The occurrence of $K_3FeMo_4O_{15}$ [28–30] gave grounds to expect formation of similar compounds with a different structure in rubidium and cesium containing systems. Such a proposal was supported experimentally when double polymolybdates $M_3FeMo_4O_{15}$ (M=Rb, Cs) were grown as a result of attempts to prepare single crystals of $M_5Fe(MoO_4)_4$. The compositions of the new compounds were recognized from X-ray structure data. Mono-phase polycrystalline samples of $M_3FeMo_4O_{15}$ (M=Rb, Cs) were prepared by annealing of the reaction mixtures M_2MoO_4:$Fe_2(MoO_4)_3$:MoO_3=3:1:2 at 450–500 °C for 80 h.

Revealing, synthesis, and XRD characterization of $M_3FeMo_4O_{15}$ (M=Rb, Cs) allow us to interpret properly the data obtained for the systems M_2MoO_4–$Fe_2(MoO_4)_3$ (M=Rb, Cs). A common subsolidus diagram of the phase fields of the systems is shown in Fig. 1, and an example of the XRD phase analysis for one sample of the system Rb_2MoO_4–$Fe_2(MoO_4)_3$ is given in Table 1.

As seen from the XRD results of the systems under consideration (Fig. 1), there are two three-phase ranges, which extend from 83.3 to 64.3 mol% and from 64.3 to 50 mol% M_2MoO_4, respectively. The phase composition of the first is Fe_2O_3, $M_3FeMo_4O_{15}$,

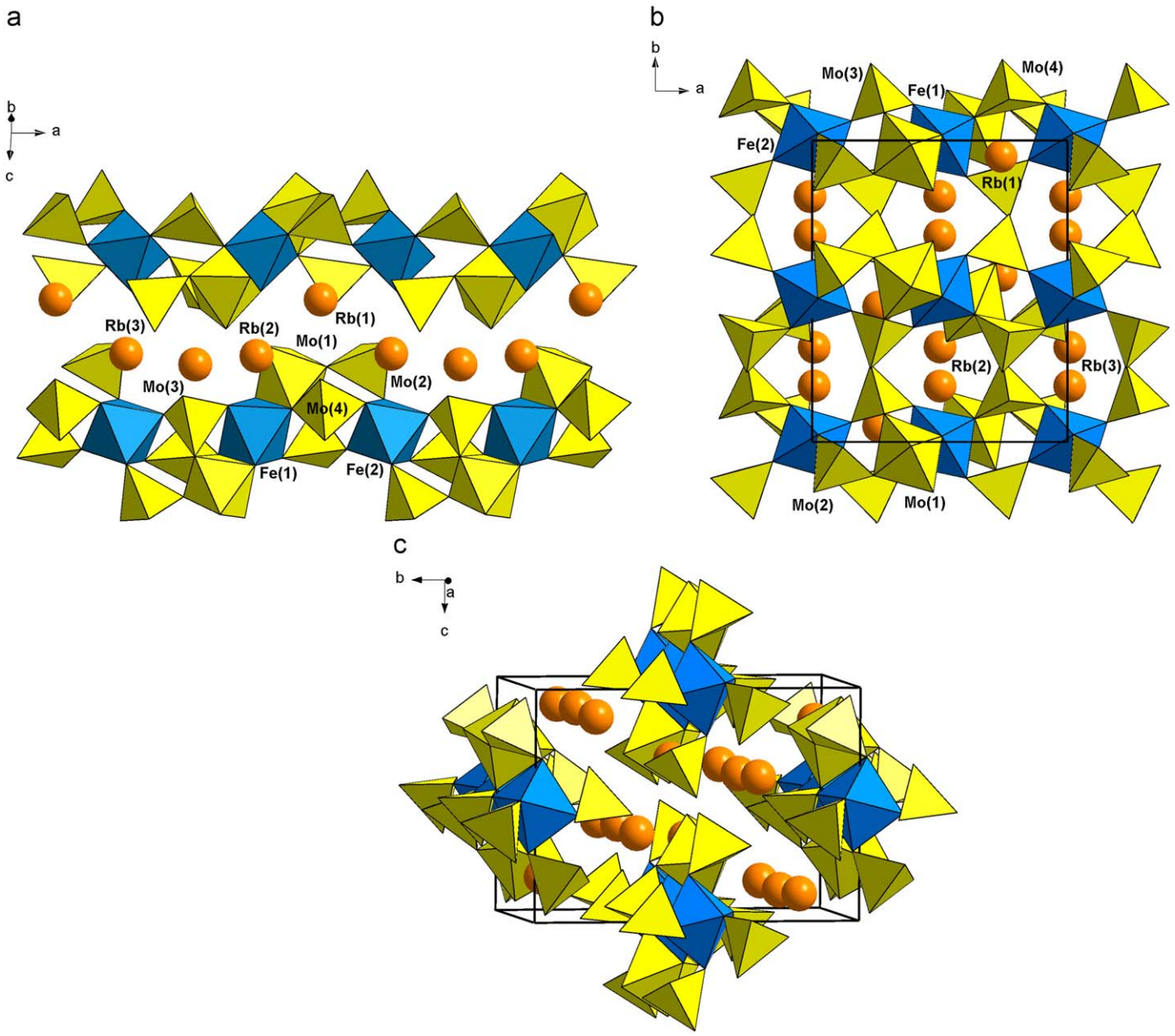

Fig. 4. The structure of $Rb_3FeMo_4O_{15}$: (a) chains of FeO_6 octahedra, $Mo(1)O_6$ octahedra, and MoO_4 tetrahedra; (b) projection of the structure along the c axis; (c) general view of the structure approximately along the a axis.

and $M_5R(MoO_4)_4$; the second range involves $M_3FeMo_4O_{15}$, $MFe(MoO_4)_2$, and Fe_2O_3. This indicates a partial deviation from quasibinarity for the systems M_2MoO_4–$Fe_2(MoO_4)_3$ due to the more complex metathesis reaction as compared to (1):

$$9M_2MoO_4+5Fe_2(MoO_4)_3\rightarrow 6M_3FeMo_4O_{15}+2Fe_2O_3 \quad (2)$$

Therefore, the joins M_2MoO_4–$Fe_2(MoO_4)_3$ (M=Rb, Cs) have to be considered in terms of the ternary oxide systems M_2O–MoO_3–Fe_2O_3 (M=Rb, Cs). Fig. 2 shows one of the possible variants of a partial triangulation of the system Rb_2O–MoO_3–Fe_2O_3, which agrees with the experimental results obtained for the Rb_2MoO_4–$Fe_2(MoO_4)_3$ section. Taking into account the presence of $K_3FeMo_4O_{15}$ [28–30], a similar reaction would be expected for the system K_2MoO_4–$Fe_2(MoO_4)_3$ but this requires an experimental evidence.

A partial non-quasibinarity of the systems M_2MoO_4–$Fe_2(MoO_4)_3$ revealed by us, is the first experimental evidence of non-binary character of the systems M_2MoO_4–$R_2(MoO_4)_3$ with heavy alkali metals. A similar phenomenon was observed for the systems Na_2MoO_4–$R_2(MoO_4)_3$ (R=Al, Cr, Fe) in the Na_2MoO_4 rich range [6]. A complex and partially non-quasibinary character of the interactions in some systems M_2WO_4–$R_2(WO_4)_3$ and M_2XO_4–AXO_4 (M=heavy alkali metals, A and R are bivalent and trivalent metals, respectively, X=Mo, W) is also confirmed in [37–41].

3.2. Crystal structures of $M_3FeMo_4O_{15}$ (M=Rb, Cs)

Crystal and structure refinement data for both compounds are given in Table 2, selected interatomic distances are listed in Tables 3 and 4. The atomic coordinates, anisotropic atomic displacement parameters, and further details of the crystal structure investigations can be obtained from the Fachinformationszentrum Karlsruhe, 76344 Eggenstein-Leopoldshafen, Germany, (fax: (49) 7247-808-666; e-mail: crysdata@fiz.karlsruhe.de) on quoting the depository numbers CSD 420802 and 420803 for $Rb_3FeMo_4O_{15}$ and $Cs_3FeMo_4O_{15}$, respectively.

The asymmetric unit of $Rb_3FeMo_4O_{15}$ structure is shown in Fig. 3. In the structure, the Fe(1) and Fe(2) atoms are in special positions at the inversion centers and have usual octahedral coordination. The remaining atoms are in general fourfold positions. The Mo(1) atom has a distorted (5+1) octahedral coordination with one oxygen atom separated by 2.535(3) Å and the remaining Mo(1)–O 1.715(2)–2.267(2) Å, whereas the Mo(2) and Mo(3) atoms are tetrahedrally coordinated. The coordination of Mo(4) may be considered in the first approximation as tetrahedral with Mo(4)–O 1.701(2)–1.890(2) Å but the presence of the distance Mo(4)–O(4) 2.553(4) Å, strictly speaking, makes us to describe the Mo(4) coordination as trigonal-bipyramidal (4+1).

In the structure, the $Fe(1)O_6$ octahedra share two opposite edges with two $Mo(1)O_6$ octahedra linked to the $Fe(2)O_6$ octahedra through the common oxygen vertices with bridged MoO_4 tetrahedra to form the chains running along the a axis (Fig. 4a). The unit cell contains two such symmetrically equivalent chains passing through the midpoints of the b and c edges (Fig. 4b). Three sorts of Rb cations are in between the chains. The Rb(1) and Rb(2) atoms are 10-fold coordinated, while the Rb(3) has a ninefold coordination.

The asymmetric unit of $Cs_3FeMo_4O_{15}$ structure is shown in Fig. 5. In the structure, the Fe(1) and Fe(2) atoms are situated at the inversion centers and are octahedrally coordinated by oxygen atoms. The remaining atoms are located in general positions. The Mo(1) atom has a distorted (4+2) octahedral coordination with four oxygen atoms at distances Mo(1)–O 1.719(10)–1.987(9) Å and two oxygen atoms separated by 2.337(10) and 2.494(11) Å. The Mo(2) and Mo(3) atoms are tetrahedrally coordinated. The Mo(4) coordination may be considered as tetrahedral with

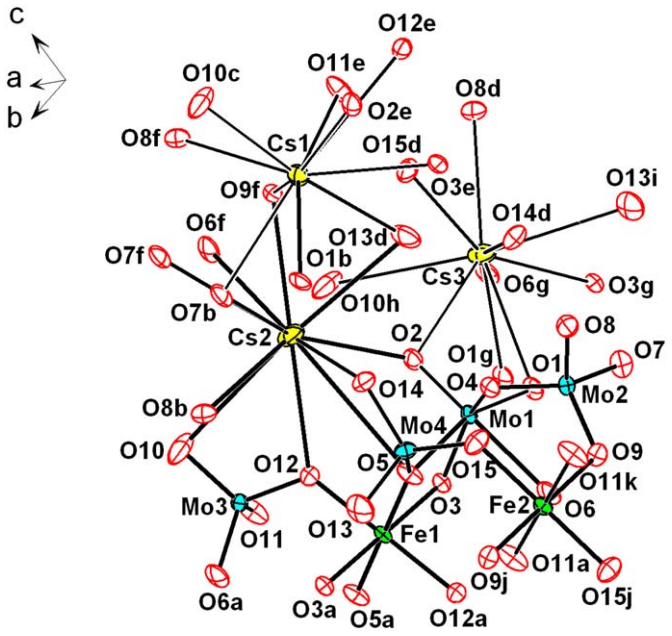

Fig. 5. The asymmetric unit of $Cs_3FeMo_4O_{15}$ structure. Atomic displacement ellipsoids are shown at 50% probability level. Symmetry codes correspond to those given in Table 4, the additional codes: (j) $-x$, $-y+1$, $-z$, (k) $x-1$, y, z.

Mo(4)–O 1.718(10)–1.858(10) Å though the weak bond Mo(4)–O(4) 2.675(9) Å formally makes it trigonal-bipyramidal. All cesium atoms are 10-fold coordinated.

The structures of $Cs_3FeMo_4O_{15}$ and $Rb_3FeMo_4O_{15}$ are very similar. In the both compounds, the coordination polyhedra of Mo and Fe atoms form polyhedral chains with very close configurations (see Figs. 4a and 6a). The stackings of the polyhedral chains are also similar in the first approximation (Figs. 4b, c and 6b, c). A large similarity of the structures appears in the close unit cell parameters (taking into account the transposition of their b and c axes) and the atomic coordinates, which were put to a comparable numeration in the both structures. However, the compounds are not isostructural because of the different monoclinic axes and space groups. The structural differences are caused by different mutual arrangements of the neighboring polyhedral chains as it is seen in Figs. 4a and 6a. Despite a practical identity of each chain to that in the different structures (the lower chains in Figs. 4a and 6a), the neighboring chains are displaced and mutually turned in the opposite directions (the upper chains in Figs. 4a and 6a). A similar situation is observed for the structures of the orthorhombic $Na_2Mo_2O_7$ [42] and the monoclinic $Cs_2Mo_2O_7$ [43], which involve the chains of MoO_6 octahedra and MoO_4 tetrahedra of the same configuration, whereas there are significant differences in symmetry of crystals, unit cell parameters, and the coordination of alkali metal cations.

Noticeable, the structure units and motifs of the both compounds essentially differ from those in $K_3FeMo_4O_{15}$ [30]. The latter structure contains separate centrosymmetrical dimeric ions $[Fe(MoO_4)_2(Mo_2O_7)]_2^{6-}$, whereas structures of $M_3FeMo_4O_{15}$ (M=Rb, Cs) have a chain (but various for these two cases) character. It is clear that structure changes between these three structures are caused by various ways of adapting anionic radicals of FeO_6 octahedra and molybdenum–oxygen polyhedra to different-sized alkali cations. At the same time, in spite of such differences, the formation of isoformular stable compounds $M_3FeMo_4O_{15}$ (M=K, Rb, Cs) in the corresponding ternary systems M_2O–MoO_3–Fe_2O_3 may mean existence of similar polymolybdates in the analogous systems with other trivalent metals.

The compositions close to $M_3FeMo_4O_{15}$ (M=K, Rb, Cs) have isotypic compounds $K_4A^{2+}Mo_4O_{15}$ (A^{2+}=Mg, Co, Cd) [44,45] with

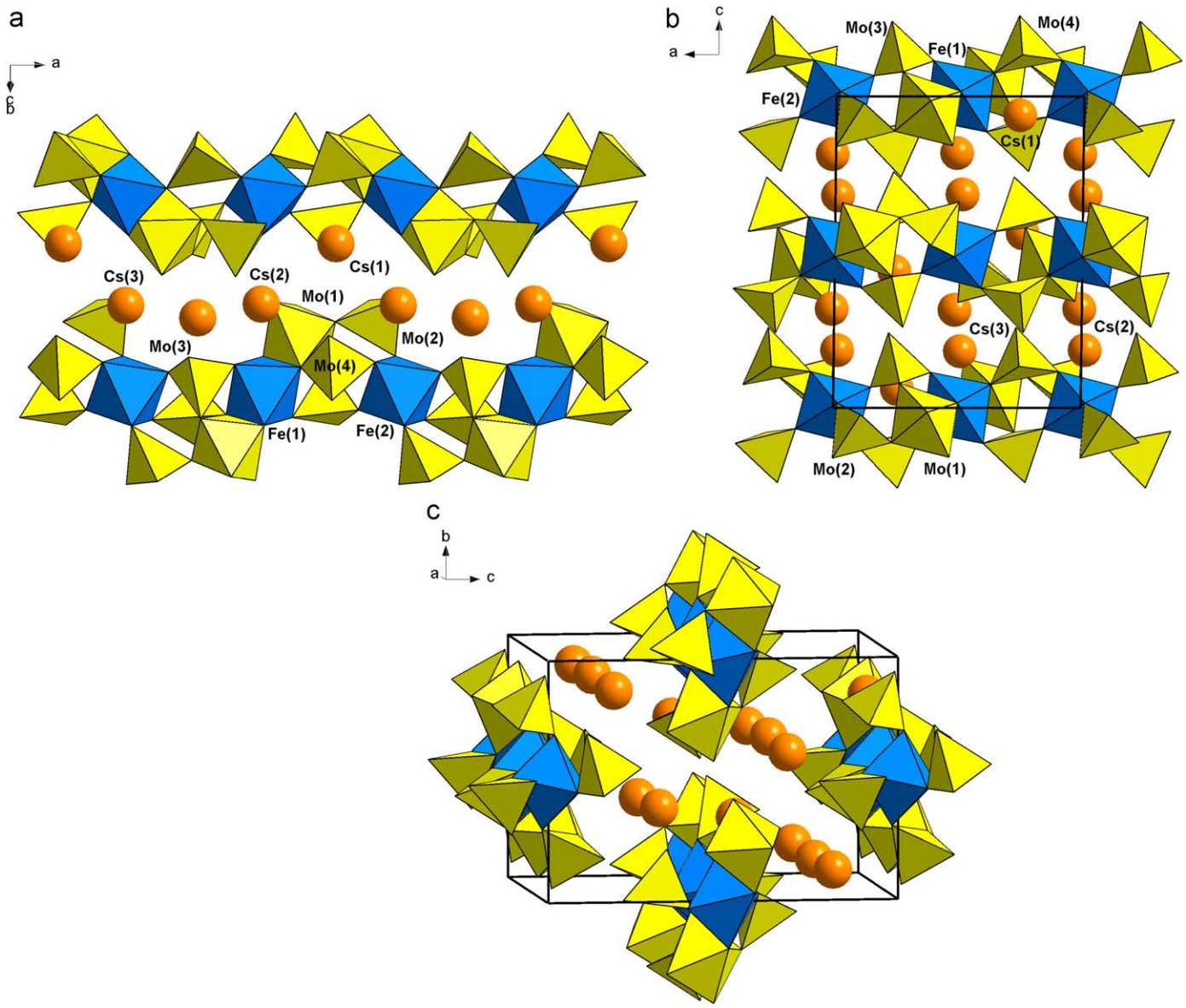

Fig. 6. The structure of $Cs_3FeMo_4O_{15}$: (a) chains of FeO_6 octahedra, $Mo(1)O_6$ octahedra, and MoO_4 tetrahedra; (b) projection of the structure along the *b* axis; (c) general view of the structure approximately along the *a* axis.

a layered glaserite-like structure, which contains face-sharing $A^{2+}O_6$ and MoO_6 octahedra and bridged MoO_4 tetrahedra. In addition, in the systems K_2O–MoO_3–$A^{2+}O$, there are other double polymolybdates $K_{10}A^{2+}Mo_7O_{27}$ (A^{2+}=Mg, Mn, Co) [46] and $K_6CoMo_5O_{19}$ [45]. This could confirm a relative abundance of complex polymolybdates within the systems M_2O–MoO_3–$A^{2+}O$ ($R^{3+}{}_2O_3$). The thermodynamic stability of these compounds is just a reason originating the above mentioned non-quasibinarity of the systems M_2MoO_4–$Fe_2(MoO_4)_3$ (M=Rb, Cs) and A_2MoO_4–$MnMoO_4$ (A=Na, K, Rb, Cs) [39–41]. This should attract attention to the further exploring phase formation and phase relations in the systems M_2O–MoO_3–$A^{2+}O$ ($R^{3+}{}_2O_3$) followed by the study of crystal structures and properties of double polymolybdates revealed in the systems.

Acknowledgments

The authors are grateful to Dr. Dmitry Yu. Naumov and Dr. Natalia V. Kuratieva for collecting and processing X-ray single-crystal diffraction data on a Bruker-Nonius X8 Apex CCD diffractometer. The authors thank Mrs. Tamara S. Yudanova for translating the paper from Russian. This work was partly supported by the Russian Foundation for Basic Research, Grant no. 03–08–00384.

Appendix A. Supplementary material

Supplementary data associated with this article can be found in the online version at doi:10.1016/j.jssc.2010.01.008

References

[1] A.A. Kaminskii, Laser Crystals. Their Physics and Properties, second ed., Springer Series in Optical Sciences, vol. 14, Springer, Berlin, Germany, 1990.
[2] V.K. Trunov, V.A. Efremov, Yu.A. Velikodny, Kristallokhimiya i Svoistva Dvoinykh Molibdatov i Volframatov [Crystal Chemistry and Properties of Double Molybdates and Tungstates], Nauka, Leningrad, 1986, 173pp. (in Russian).

[3] A.A. Evdokimov, V.A. Efremov, V.K. Trunov et al., Soedineniya Redkozemelnykh Elementov. Molibdaty. Volframaty [Rare-earth Compounds. Molybdates, Tungstates], Nauka, Moscow, 1991, 267pp. (in Russian).
[4] V.A. Isupov, Ferroelectrics 321 (2005) 63.
[5] V.L. Butukhanov, Ph.D. Thesis (Chemistry), Donetsk, USSR, 1974, 134pp.
[6] V.K. Trunov, Yu.A. Velikodny, Izv. Akad. Nauk USSR Neorg. Mater. 8 (1972) 881.
[7] V.K. Trunov, V.A. Efremov, Zh. Neorg. Khim. 16 (1971) 2026.
[8] P.V. Klevtsov, Kristallografiya 15 (1970) 797.
[9] P.V. Klevtsov, L.P. Kozeeva, R.F. Klevtsova, Zh. Neorg. Khim. 20 (1975) 2999.
[10] E.V. Sinyakov, E.F. Dudnik, T.M. Stolpakova, O.L. Orlov, Ferroelectrics 21 (1978) 579.
[11] G.A. Smolensky, S.D. Prokhorova, I.G. Siny, et al., Ferroelectrics 26 (1980) 677.
[12] M. Maczka, A. Pietraszko, G.D. Saraiva, et al., J. Phys. Condens. Matter 17 (2005) 6285.
[13] L.E. Svistov, A.I. Smirnov, L.A. Prozorova, et al., Phys. Rev. B. 67 (2003) 094434/1.
[14] S.A. Klimin, M.N. Popova, B.N. Mavrin, et al., Phys. Rev. B Condens. Matter Mater. Phys. 68 (2003) 174408/1.
[15] L.A. Prozorova, L.E. Svistov, A.I. Smirnov, et al., J. Magn. Magn. Mater 258–259 (2003) 394.
[16] L. Sebastian, Y. Piffard, A.K. Shukla, et al., J. Mater. Chem. 13 (2003) 1797.
[17] M. Alvarez-Vega, U. Amador, M.E. Arroyo-de Dompablo, J. Electrochem. Soc. 152 (2005) A1306.
[18] ICDD PDF-2 Data Base, Card # 52-645.
[19] B.I. Lazoryak, V.A. Efremov, Kristallografiya 32 (1987) 378.
[20] M. Wierzbicka-Wieczorek, U. Kolitsch, E. Tillmanns, Z. Kristallogr. New Cryst. Struct. 224 (2009) 151.
[21] A. Van der Lee, M. Beaurain, P. Armand, Acta Crystallogr. C 64 (2008) i1.
[22] R.F. Klevtsova, P.V. Klevtsov, Kristallografiya 15 (1970) 953.
[23] R.F. Klevtsova, Dokl. Akad. Nauk USSR 221 (1975) 1322.
[24] B.G. Bazarov, R.F. Klevtsova, Z.T. Bazarova, et al., Zh. Neorg. Khim. 51 (2006) 1190.
[25] T. Inami, J. Solid State Chem. 180 (2007) 2075.
[26] R.F. Klevtsova, S.A. Magarill, Kristallografiya 15 (1970) 710.
[27] R.G. Tissot, M.A. Rodriguez, D.L. Sipola, J.A. Voigt, Powder Diffr. 16 (2001) 92.
[28] A. Kirfel, K. Petrov, St. Karagiozova, Z. Kristallogr. 160 (1982) 153.
[29] Z.A. Solodovnikova, S.F. Solodovnikov, in: All-Russian Scientific Conference devoted to the 70th Anniversary of Prof. M.V. Mokhosoev, Ulan-Ude, Russia, 27–30 June 2002, Book of Abstracts, p. 82.
[30] M. Maczka, A. Pietraszko, W. Paraguassu, et al., J. Phys. Condens. Matter 21 (2009) 095402 (8pp.).
[31] E.I. Get'man, T.A. Ugnivenko, N.G. Kisel', E.I. Stambler, Zh. Neorg. Khim. 21 (1976) 3394.
[32] V. Massarotti, G. Flor, A. Marini, J. Appl. Cryst. 14 (1981) 64.
[33] SAINT (Version 7.03), SADABS (Version 2.11), Bruker AXS Inc., Madison, Wisconsin, 2004.
[34] G.M. Sheldrick, SHELX-97, Release 97-2, University of Goettingen, 1997.
[35] ICDD PDF-2 Data Base, Card # 52-646.
[36] ICDD PDF-2 Data Base, Card # 33-664.
[37] Yu.A. Velikodny, Ph.D. Thesis (Chemistry), Moscow, USSR, 1975, 121pp.
[38] M.V. Mokhosoev, F.P. Alekseev, Zh. Neorg. Khim. 29 (1984) 499.
[39] S.F. Solodovnikov, Z.A. Solodovnikova, P.V. Klevtsov, E.S. Zolotova, Zh. Neorg. Khim. 39 (1994) 1942.
[40] S.F. Solodovnikov, Z.A. Solodovnikova, P.V. Klevtsov, E.S. Zolotova, Zh. Neorg. Khim. 40 (1995) 223.
[41] S.F. Solodovnikov, Z.A. Solodovnikova, P.V. Klevtsov, E.S. Zolotova, Zh. Neorg. Khim. 40 (1995) 305.
[42] M. Seleborg, Acta Chem. Scand. 21 (1967) 499.
[43] Z.A. Solodovnikova, S.F. Solodovnikov, Acta Crystallogr. C 62 (2006) i53.
[44] S.F. Solodovnikov, E.S. Zolotova, Z.A. Solodovnikova, J. Struct. Chem. 38 (1997) 83.
[45] J.M. Engel, H. Ehrenberg, H. Fuess, Acta. Crystallogr. C 61 (2005) i111.
[46] S.F. Solodovnikov, R.F. Klevtsova, L.A. Glinskaya, et al., J. Struct. Chem. 38 (1997) 426.